JOURNAL OF AGRICULTURAL AND FOOD CHEMISTRY

Influence of the Spatial Organization of the Perimysium on Beef Tenderness

LAURENCE SIFRE,*,† PHILIPPE BERGE,† ERWAN ENGEL,† JEAN-FRANÇOIS MARTIN,† JEAN-MARIE BONNY,† ANNE LISTRAT,‡ RICHARD TAYLOR,† AND JOSEPH CULIOLI†

Quality of Animal Products Unit and Herbivore Research Unit, Institut National de Recherche Agronomique, Theix 63122 Saint-Genès-Champanelle, France

The spatial distribution of the intramuscular connective tissue (IMCT) in four types of beef muscle (*Biceps femoris*, *Infraspinatus*, *Longissimus thoracis*, and *Pectoralis profundus*) was examined using histology and magnetic resonance imaging (MRI). The surface and the length of the IMCT and the surface of the myofiber bundles were evaluated by image analysis. The texture of the cooked meat from these muscles was measured both instrumentally by a compression test and by sensory analysis. The relationship between muscle structure and meat texture was studied by general discriminant analysis. The models obtained could assign correctly up to 87% of the samples to two tenderness classes. Histology and MRI provided complementary information about the microscopic and macroscopic IMCT structures, respectively. Both were necessary to predict sensory tenderness whereas only the MRI measurements were necessary to predict instrumental toughness. Tough muscles had smaller MRI myofiber bundles (0.7−1 mm radius) than tender muscles.

KEYWORDS: Connective tissue; meat; tenderness; muscle structure; image analysis

INTRODUCTION

Tenderness is one of the main eating quality attributes, which determine the consumer acceptance for beef (*1*). This attribute depends mostly on the properties of the two main structural constituents of muscle tissue, the myofibers and the intramuscular connective tissue (IMCT), and on the interactions between the two. After animal slaughtering and following rigor development, the myofibers undergo a proteolytic breakdown (the so-called aging process) causing the progressive tenderization of beef meat. When the aging conditions are optimal (e.g., relatively long storage time and adequate chilling conditions), the toughness of uncooked meat depends mainly on the properties of the IMCT, whereas the contribution of the myofibers becomes minimal. During cooking, the heat denaturation process affects both the structure and the properties of myofibers and IMCT; that is, it increases considerably the toughness of the myofibrillar compartment and decreases that of IMCT (*2*). However, the IMCT still contributes to the toughness of cooked meat, depending upon the cooking conditions (e.g., temperature, duration) (*2*), the amount of collagen (the main IMCT component), the heat stability of this protein, and the spatial organization of the IMCT within the muscle (*3*). Previous studies have shown that the relationship between collagen content and meat tenderness is poor (*3*). In addition, collagen heat stability alone poorly explains the variations of meat toughness (*3*). Thus, the structure of IMCT, including its spatial distribution in the muscle and its composition, may play a significant role in the toughness of fully aged meat. IMCT is organized in three compartments: (i) the endomysium that surrounds the individual skeletal muscle fibers, (ii) the perimysium that surrounds groups of muscle fiber bundles, and (iii) the epimysium that surrounds the whole muscle (*3*). The epimysium is generally removed by the butcher, and it is thus not involved in meat texture. The chemical and morphological characteristics of the endomysium are slightly variable across muscle types and animal species (*3*). Because the perimysium is, in proportion, the major and most variable IMCT compartment, one may presume that the contribution of IMCT to the variations of cooked meat tenderness is predominantly due to the properties of the perimysium. Several authors studied the influence of perimysium thickness on meat tenderness (*4*, *5*) or that of the size of the fascicles bundles delimited by the perimysium (*6*−*9*). They associated thin IMCT and small myofiber bundles to tender meat. However, previous studies had not had the appropriate tools to evaluate objectively and quantitatively the parameters of the distribution of the entire IMCT network. Today, such measurements can be carried out automatically using image analysis. In the present work, different imaging modalities have been used to acquire images of IMCT, such as visible images of stained muscle sections and magnetic resonance imaging (MRI) of fresh muscle samples. Attributes of image analysis describing the perimysium and the organization of fascicles in the muscle (raw meat) have been correlated to textural traits measured on cooked meat (instrumental and

* To whom correspondence should be addressed. Tel: +33.4.73.62.46.96. Fax: +33.4.73.62.40.88. E-mail: lmaunier@clermont.inra.fr.
† Quality of Animal Products Unit.
‡ Herbivore Research Unit.

10.1021/jf0508910 CCC: $30.25
Published on Web 09/16/2005

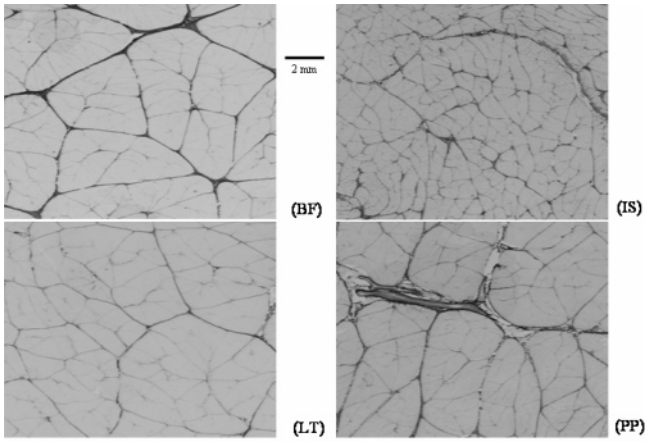

Figure 1. Transverse histological sections of the four muscle types stained with Sirius Red: BF, IS, LT, and PP. Black lines are connective tissue and lipids. Myofibers are shown in gray.

sensory assessments), to determine the relationships between IMCT structure and meat toughness.

MATERIALS AND METHODS

Animals and Samples. Eight 5 year old Charolais cull cows were slaughtered in a commercial abattoir. Four muscles, *Biceps femoris* (BF), *Infraspinatus* (IS), *Longissimus thoracis* (LT), and *Pectoralis profundus* (PP), were excised from both sides of each carcass 24 h postmortem. Histological samples were removed, and the remainder of the muscles was aged at 4 °C until 21 days postmortem. After aging, the muscles were cut into 4 cm thick steaks, which were vacuum-packed and kept frozen at −20 °C until they were analyzed.

Control Measurements. The aging state of the 1 cm^2 section samples was evaluated on raw meat as the stress (C20, N/cm^2) reached at a 20% compression strain according to the method of Lepetit and Buffière (*15*), using a three-sided compression cell (which avoided transverse deformation of the sample) mounted on an Instron 4501 Universal Testing Machine (Instron Corp., Canton, MA). A minimum of 10 replicates per steak was analyzed. Sarcomere length was measured to assess the state of contraction of meat induced by postmortem chilling. Muscle samples were homogenized in a buffer solution containing 0.25 M KCl, 0.29 M orthoboric acid, and 0.005 M EDTA, according to Cross et al. (*16*), without glutaraldehyde. A suspension was then mounted on a slide and observed with a Polyvar optic microscope (Reichert-Jung), in oil immersion at a 125-fold magnification. The images were acquired using Visilog 5.4 software. They showed isolated myofibers and the succession of the *Z*-lines, which define the sarcomere length.

Histology. Muscle samples of 20 × 20 × 10 mm^3 were cut parallel to myofiber orientation, the largest section being perpendicular to the main myofiber orientation, and frozen in isopentane chilled at −160 °C by liquid nitrogen. They were cut to make 10 μm thick cross-sections approximately 2 cm^2 with a cryostat (Cryo-star HM560MV, Microm international GmbH, Germany). Perimysial tissue was stained with red Sirius dye (*10*), which colors IMCT red and muscle fibers yellow (respectively, black and gray in **Figure 1**). Digital images (512 × 512) were obtained using a transmitting light box and a CCD camera JAI CV-M300 coupled with a macroscopic objective (2-fold magnification) leading to a pixel size of 27 × 27 μm^2. The quality of the images was improved by eliminating light reflection using black masks. A green filter was fixed on the objective in order to improve the contrast. All images were digitized using the same conditions of lighting and magnification and processed using Visilog 5.4 software (Noesis, 6-8 rue de la Réunion, Courtaboeuf, France).

MRI. Samples of 50 × 50 × 100 mm^3 were cut according to myofiber orientation (parallel to the longest dimension of the fibers) from each of the muscles studied. Twenty MR images were acquired perpendicular to the myofiber orientation at high field (4.7 T) using a susceptibility-weighted sequence according to the protocol described by Bonny et al. (*11*). The sequence parameters were optimized for obtaining a voxel size of 100 × 100 × 500 μm^3 in an acquisition time of 5 h and 41 min (**Figure 2**). The MR images were averaged two by two to obtain 10 mean images. The two mean images at both borders of the samples were eliminated to limit heterogeneity problems so only six mean images were processed.

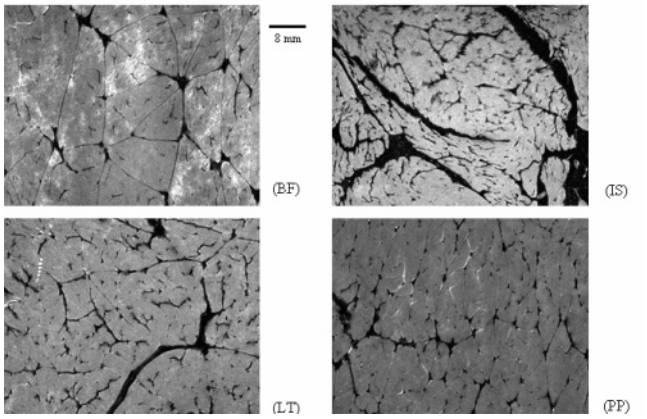

Figure 2. Transverse sections of the four muscle types in MRI: BF, IS, LT, and PP. Black lines are connective tissue and lipids. Myofibers are stained in gray.

Image Processing. Both histological and MR images showed unimodal histograms. So, they were processed by adaptive thresholding based on probabilistic maps (*12*). The confidence level, which is the degree of freedom of the algorithm, was set to 80% in order to extract only the thickest segments. This confidence level was used to segment pixels whose probability of being in perimysium was high (error lower than 20%). After segmentation, the surface of the perimysium network was measured as the number of segmented pixels. The length was determined after skeletization of the segmented perimysium and measured as the number of pixels of the resultant skeleton. These data were expressed as the percentage of pixels in the image.

Then, the granulometry of the fascicles delimited by perimysium, i.e., the distribution of the fascicle size, was computed using a morphological operator. The binary image was treated as a collection of grains (fascicles), and the grains were sieved though a filter of increasing mesh size (*13*). The negatives of the segmented images (fascicles considered as objects) were processed by applying successive openings with a hexagonal structural element of increasing radius. The hexagon was kept if it was included in a fascicle. Counting of the number of hexagons after each "sieving" provided a size distribution of distinct fascicles. Moreover, only the largest size of hexagon was kept of a given fascicle to estimate the size of the fiber fascicles. Granulometry variables called G_i for MR images and H_i for histological images were quantified from the granulometry curves, which expressed the total surface occupied by hexagons of a radius equal to *i* times the pixel size (**Figure 3**).

Instrumental Texture Evaluation. Steaks were thawed overnight at 4 °C (±1 °C). They were then vacuum-packaged and subjected to fast preheating in a 20 °C water bath heated in a microwave oven up to 60 °C (approximate duration 10 ± 1 min). The samples were then immediately transferred into a second water bath at 65 °C for further cooking at this temperature for 30 min. After they were rapidly cooled in water at 15 °C, the cooked steaks were left to equilibrate to room temperature, unpacked, and cut into 1 cm^2 cross-section samples, with muscle fibers parallel to the longitudinal axis of the sample (approximate length 30 mm). The compression was performed perpendicularly to myofibers at a rate of 50 mm/min, and the stress (C80, N/cm^2) reached at an 80% strain was then measured (*14*). A minimum of 10 replicates per steak was analyzed.

Sensory Analysis. The steaks were thawed overnight at 4 °C (±1 °C) and cooked in the same way as those used for the instrumental texture measurement and then stored at −20 °C until further analysis. The day of the assessment, they were thawed, equilibrated at room temperature, and cut into 1.5 cm cubes. Ten panelists, experienced in texture profiling of meat samples, participated in four training sessions

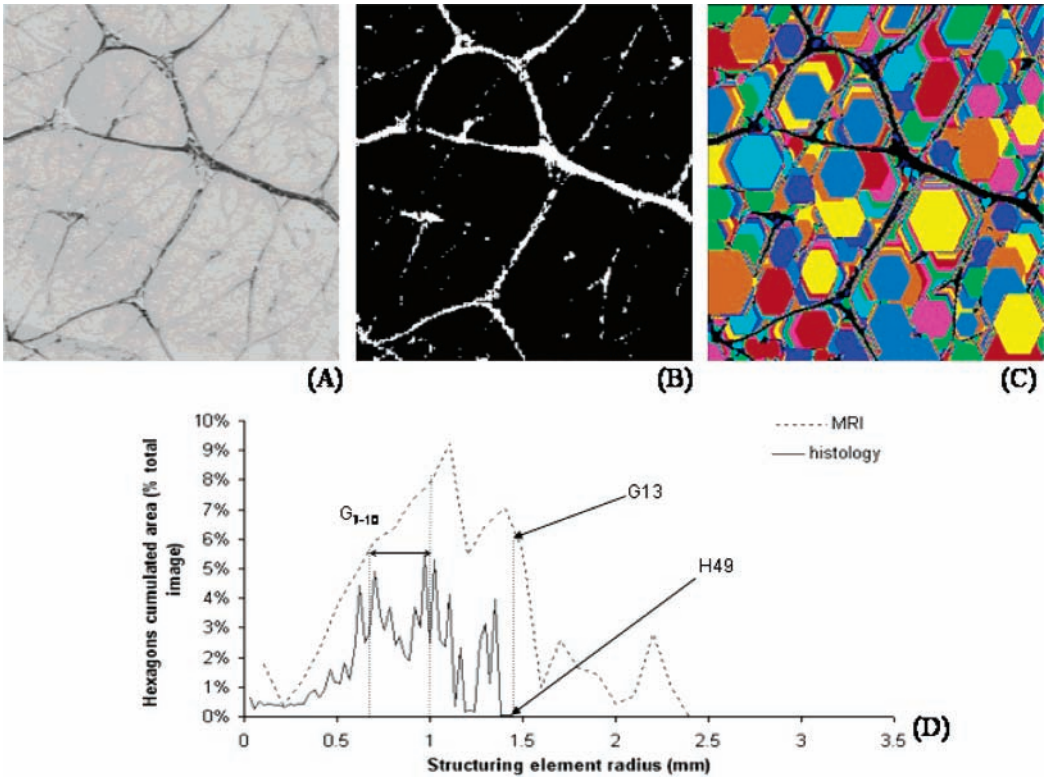

Figure 3. Example of granulometry on a muscular image. (**A**) Original histological image, (**B**) segmented histological image, (**C**) granulometric histological image, and (**D**) granulometric curves. Hexagons with the same radius appear with the same color. H_{49} was the higher granulometric size for histological images and corresponded to G_{13} on MR images. G_{7-10} was the granulometric size on MRIs, which appeared in all best models to predict instrumental toughness, sensory tenderness, and collagen content.

to generate selected descriptive terms and to become familiar with the type of meat and the sensory descriptors. They evaluated each sample twice according to a monadic presentation in Latin square. In one session, the four muscles from one animal were evaluated twice. Each panelist had to taste eight plates containing three none-reheated pieces of one muscle from one animal. All of the sensory evaluation tests were carried out under white light at 20 °C. Panelists were asked to rate each sample for the intensity of the following attributes in the mouth: tender, compact, juicy, residue amount, supple, sticking, floury, and elastic, using a nonstructured 10 point scale with score "0" equivalent to not perceptible and score "10" equivalent to extremely intense. These attributes were chosen because they were discriminating for muscle type ($p < 0.05$) during the training session. The consensus among the panelists was tested using a mixed model with panelists as a random effect. The mean of the 10 panelists for each sample was used for data analysis.

Collagen Content Determination. Collagen content was determined on all of the muscles studied. It was calculated from the hydroxyproline concentration (collagen = 7.5 × OH−Pro) determined on five replicates of muscle homogenate using the method of Bergman and Loxley (*17*) modified by Bonnet and Kopp (*18*) and expressed in mg of collagen per g of fresh muscle. The insoluble collagen content was also determined applying the same procedure on the residue obtained after heating the meat sample in a 0.02 M Tris-HCl, 0.23 M NaCl, pH 7.4, buffer solution (1:5 w/v) at 65 °C for 30 min and subsequently discarding the heat soluble fraction as described by Bonnet and Kopp (*18*). Collagen heat solubility was calculated as the percentage of heat soluble collagen (100 − insoluble collagen) in total collagen.

Statistical Analysis. The effect of muscle type on variables including C20, sarcomere length C80, tenderness, collagen content, and its thermal stability and IMCT network measurements was studied by a one-way analysis of variance (ANOVA) using a general linear model procedure (model: dependent variable = muscle type). When significant differences were found ($p < 0.05$), mean values calculated for each muscle type were compared using a Neuman−Keuls multiple comparison test. These analyses were performed using SAS software release 8.1 (SAS Institute Inc., Cary, NC). The texture profile results, obtained by sensory assessment, were described by principal component analysis (PCA) using the Statistica software release 6.1 (Statsoft, France).

The relationship between the predicted variables (C80, sensory tenderness, and collagen content) and predictive variables including the "image" variables (surface or length of the network, granulometry measurements from histology and MR images) and collagen content was determined using the Statistica software. The "image" variables had to be sorted because of the very high number of granulometry variables. First, the granulometry variables that had 10 or more zero values out of the 32 observations were excluded. A second step consisted of clustering the remaining variables of granulometry by a *k*-means algorithm according to their mutual correlation and to make groups of granulometry variables representing consecutive sizes. The value associated with the clustering of variables G_i to G_j was calculated as $G_{i-j} = G_i + G_{i+1} + ... + G_{j-1} + G_j$.

For each predicted variable (C80, sensory tenderness, and collagen content), the samples were ranked into two classes (e.g., tough vs tender) determined by the *k*-means algorithm.

One-way ANOVA was performed on each predictive variable (collagen content, network, and granulometry variables measured on histology and NMR images) according to the model predictive variable = class, where class is one of the two groups previously determined for C80, tenderness, and collagen content. Only discriminative variables ($p < 0.05$) were used for studying their relationship with predicted variables by general discriminant analysis (GDA). It applied the methods of the general linear model to the discriminant function analysis problem. Discriminant function analysis was used to determine which variables discriminate between two or more naturally occurring groups (*19*).

The relationship between the predicted variables and the IMCT characteristics was determined by GDA. The 32 observations were divided randomly into three groups: a learning group ($n = 16$), a validation group ($n = 8$), and a test group ($n = 8$). The best subset algorithm was used on the learning group to select models comprising two or three variables. The best subset of variables was selected on

Table 1. Means and Standard Deviations of the Texture Measurements of the Four Muscle Types: BF, IS, LT, and PP[a]

sarcomere length (μm)	20% compression raw meat (N/cm^2)	80% compression cooked meat (N/cm^2)	sensory tenderness
BF (2.0 ± 0.2) b	BF (2.9 ± 0.9) ab	BF (126.6 ± 37.2) b	BF (4.1 ± 1.5) b
IS (2.4 ± 0.3) ab	IS (3.9 ± 1.5) a	IS (85.1 ± 13.5) c	IS (5.7 ± 1.5) a
LT (1.9 ± 0.4) b	LT (2.4 ± 0.7) b	LT (97.8 ± 10.8) c	LT (6.1 ± 1.4) a
PP (2.7 ± 0.5) a	PP (4.1 ± 1.3) a	PP (174.2 ± 37.6) a	PP (4.1 ± 1.5) b

[a] Different letters in the columns indicate significant differences between muscle types ($p < 0.05$) with Neuman–Keuls test.

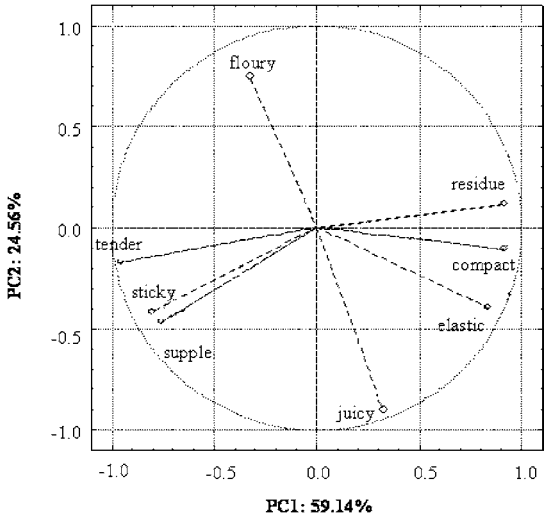

Figure 4. PCA of the sensory attributes. The plan defined by the first and second PCs explains almost 84% of the variance.

the "learning + validation" data set according to a cross-validation algorithm where the misclassification rate was chosen as the main criterion of ranking between the models. The quality of the chosen model was determined by the percentage of correctly classified individuals in the test group.

RESULTS AND DISCUSSION

Texture Assessment. The stress values for raw meat obtained at 20% compression strain (**Table 1**) showed that all meat samples were fully aged (C20 < 5 N/cm^2). No significant difference was observed between animals ($p > 0.05$). Under such circumstances, one could consider that the myofibrillar resistance and its variability were minimal. The range in sarcomere lengths (1.9−2.7 μm) was consistent with that found in the literature for the corresponding muscle types in normal contraction state (*20*, *21*). Thus, it could be assumed that none of the samples studied had suffered cold shortening and that the within and between muscle types toughness variations would be mainly determined by differences in IMCT characteristics.

For cooked meat, three groups appeared with significantly different compression values ($p < 0.05$), with the PP muscle the toughest, the BF muscle intermediate, and the IS and LT muscles the most tender (**Table 1**). The values ranged from 85 to 174 N/cm^2 and were reasonably consistent with the results published by Kamoun and Culioli (*22*) for beef samples cooked at 55 °C for 30 min. These authors found maximal stresses in longitudinal sinusoidal configuration of 54 and 161 N/cm^2 for an 80% compression ratio for LT and PP muscles, respectively.

Among the 10 panelists, a consensus was reached on all sensory attributes, and so, they were all included into the texture profile. The plan defined by the first and second principal components (PC) explained approximately 84% of the variance generated by the texture profile of the samples (**Figure 4**). The first PC explained about 60% of the variance, and it consisted principally of the tender attribute, whereas the second PC was determined by the juicy and floury attributes. We chose to focus on tenderness, generally recognized as the most important sensory attribute for beef. The muscles could be segregated into two groups of tenderness according to their sensory scores: BF and PP as tough muscles and IS and LT as tender muscles (**Table 1**). The classification of the four muscle types according to tenderness was consistent with those previously published (*20*, *23*−*25*).

In this study, two methods were used to evaluate meat texture, an instrumental test [compression stress at 80% strain (C80)] and sensory analysis. The variations of cooked meat toughness measured by compression test are mainly related to changes in the mechanical properties of the connective tissue (*26*). As shown by Harris and Shorthose (*27)* and Shackelford et al. (*28*) or more recently by Rhee et al. (*25*), shear tests are not sensitive enough to detect connective tissue related differences in meat toughness between muscle types, because the major contribution to the mechanical resistance of cooked meat during a shear test is that of the myofibers.

The correlation between C80 and sensory tenderness ($r = -0.64$) was significant but lower than that obtained by Mathonière et al. (*29*) with beef *Semitendinosus* and *Semimembranosus* muscles cooked at 60 or 80 °C for 30 min ($r = -0.91$). However, these authors introduced other sources of variation such as aging time, cooking temperature, and muscle contraction state, in addition to muscle type, which led to a larger range of C80 compression values (from 143 to 451 N/cm^2 as compared to 85 to 174 N/cm^2 in the present study). After the cold shortened samples were removed, the range becomes similar to ours and the correlation coefficient decreased to −0.55 and −0.78 for cooking at 60 and 80 °C, respectively, the range of values being similar to that found in the present experiment.

Collagen Content and Heat Stability. The four muscles showed significantly different collagen contents ($p < 0.05$) (**Table 2**), and these were generally comparable to those reported in other studies (*20*, *21*, *30*, *31*). However, IS collagen content was lower than the values presented by Jeremiah et al. (*31*) and Mc Keith et al. (*20*) probably because we chose to discard the thick IMCT sheet, which runs across the IS muscle and can be easily cut away by the consumer before eating. Because it does not actually interfere with the mastication process, it should not to be taken into account when calculating the relationship between collagen content and sensory measures. Although the collagen contents of the four muscles were significantly different, only two groups were differentiated by sensory tenderness. The IS and LT muscles had the same tenderness ratings, but they were significantly different in collagen content (0.89 and 0.56 mg OH−proline/g fresh tissue, respectively).

The cooking (65 °C for 30 min) caused solubilization of only a very small proportion of the IMCT collagen (2−5%), with no significant difference between muscle types ($p < 0.05$; **Table 2**). These values are very low as compared to those reported by Torrescano et al. (*21*) (16.6−26%), but this discrepancy can

Table 2. Mean Values of the IMCT Characteristics of the Four Muscle Types: BF, IS, LT, and PP[a]

collagen content (mg OH-proline/ g fresh tissue)	soluble collagen (% total collagen)	histology		MRI	
		surface *e* (%)	length *e* (%)	surface *e* (%)	length *e* (%)
BF (1.09 ± 0.12) b	BF (2 ± 6) a	BF (4.6 ± 0.7) a	BF (1.6 ± 0.1) b	BF (12.8 ± 3.3) b	BF (4.7 ± 0.6) a
IS (0.89 ± 0.06) c	IS (5 ± 9) a	IS (3.7 ± 0.9) b	IS (1.8 ± 0.4) ab	IS (20.0 ± 2.6) a	IS (4.5 ± 0.6) ab
LT (0.56 ± 0.05) d	LT (4 ± 12) a	LT (2.8 ± 0.4) c	LT (1.4 ± 0.2) c	LT (12.4 ± 3.0) bc	LT (4.0 ± 0.5) c
PP (1.21 ± 0.13) a	PP (5 ± 11) a	PP (4.7 ± 0.9) a	PP (2.0 ± 0.3) a	PP (11.3 ± 2.2) c	PP (4.3 ± 0.7) b

[a] Different letters in the columns indicate significant differences between muscle types ($p < 0.05$) with Neuman–Keuls test. *e* is expressed in % of total image area.

easily be explained by the much more drastic cooking regime applied by these authors to their meat samples (90 °C for 2 h). The fact that collagen solubilization was very limited in the present experiment does not mean that this component did not undergo heat denaturation. However, one may presume that the consequences of heat denaturation, although not detectable by the collagen heat solubilization method used, were likely limited and did not have to play a significant role in determining the texture differences between the meat samples.

Histology Measurements. The staining on the histological images allowed the identification of the perimysium exclusive of lipids. Using this method, three muscle groups could be differentiated using either the surface or the length of IMCT (**Table 2**). The network of the LT muscle IMCT occupied a small area in the images (2.8%), and it had the shortest length (1.4% of total image), which is indicative of a low level of network branching. The IMCT network of the IS muscle also occupied a relatively small area (3.7%), but it had a longer length (1.8%), both traits being characteristic of a thin and branched IMCT network. The IMCT of the PP muscle was thick (4.7%) and even more branched (length equal to 2.0%), as illustrated in **Figure 1**. The IMCT of the BF muscle also occupied a large surface (4.6%), but its length was shorter than that of the PP muscle (1.6 and 2.0%, respectively). These two muscles had similar areas of IMCT, but their structures were quite different. The BF muscle had a thick IMCT network with fewer ramifications, whereas the IMCT of the PP muscle was more branched and thinner.

MRI Measurements. The MRI detected both collagenic tissue and lipids, being components of the IMCT. The signal visualized was thus slightly different from that visualized on the histological images where only the collagenic tissue was stained. By this method, the muscles were segregated into three groups according to their network surface in MRI (IS > BF, LT, and PP) and also into three groups according to their network length (BF, IS, and PP > LT). The BF muscle had an intermediate surface (12.8%) and the highest length (4.7%). At this scale, BF was the only muscle where well-defined fiber fascicles were visible in MRI (**Figure 2**). The IS muscle exhibited the highest IMCT surface (20.0%) due to the thick sheet of connective tissue running across the muscle and a high IMCT length (4.5%), which is indicative again of a high degree of branching (**Figure 2**). The LT muscle had a small IMCT surface (12.4%) and the lowest IMCT length (4.0%), thus showing that its perimysium was little developed. Actually, a large proportion of the segments of this muscle was too thin to be visualized by MRI and segmented because the perimysium occupied too small of a volume in the voxel to generate a signal. Despite the difference between the IMCT thicknesses of LT and PP muscles, these muscles had similar IMCT surface values. Indeed, the PP muscle had the smallest surface and a short length. Despite its thickness, little network was detected because of the distribution of marbling of this muscle (only located only at the fascicle junctions, **Figure 2**). Therefore, the IMCT composition could influence the generation of the signal in MRI in addition to the network thickness and the lipid content.

A relatively high correlation was found between collagen content and tenderness ($r = -0.78$). That was not surprising and could be attributed to the relatively limited extent of the heat denaturation of the IMCT components during cooking and to the extreme collagen contents exhibited by the different muscle types used (*25*, *30*). The correlation was higher between sensory tenderness and collagen content than it was between C80 and collagen content ($r = -0.78$ and $+0.64$, respectively). Because collagen content could not completely explain the texture variations of cooked meat samples, we looked for relationships between cooked meat tenderness and IMCT structure variables. Image analysis of IMCT structure was then used to classify the samples into groups of sensory tenderness, instrumental toughness, and collagen content.

Models to Predict Sensory Tenderness. The elimination of the variables showing 10 or more zero values allowed reduction of the number of granulometry variables from 48 and 70 to 27 and 49 variables for MRI and histological images, respectively. For MR images, *k*-means algorithm gave eight clusters: G_{1-4}, G_2, G_{5-6}, G_{7-10}, G_{11-13}, G_{14-17}, G_{18-21}, and G_{22-26}. Similarly, for histological images, 14 clusters were obtained as follows: H_{1-8}, H_{9-11}, H_{12-14}, H_{15-16}, H_{17-19}, H_{20-21}, H_{22-24}, H_{25-28}, H_{29-34}, H_{35-39}, H_{41-44}, H_{45}, H_{46-48}, and H_{49}. The number of clusters was higher for histological images. Indeed, the granulometric curve of the histological image had an irregular shape and required many radius lengths to be completely described, whereas the curve of the MR image showed few distinct modes and could be described with fewer variables (**Figure 3**). The cumulated areas were higher for MRI because the number of hexagon classes was smaller. In histological images, the areas occupied by most of the hexagon size classes were within a small range of values, whereas in MRI the repartition was less uniform.

The sensory tenderness value used to divide the data into two groups was 5.3. The tough group included all of the BF and PP samples and a few IS samples, and the tender group included all of the LT samples and most of the IS samples (**Figure 5**).

The one-way ANOVA analysis identified eight significant variables ($p < 0.05$) out of 27 for the tenderness class factor (**Figure 6**), the limit of significance being 20% of relative explained variance. Among these eight discriminating variables, only 2 or 3 were chosen at a time by the GDA algorithm to build the models. All of the best models with two variables, proposed by the GDA best subset algorithm, included a granulometry variable computed from MR images and a network variable computed from histological images, with balanced weights. Moreover, the models using only MRI variables or only histological variables were poorer predictors than the model based on G_{7-10} and the length of the network on histology

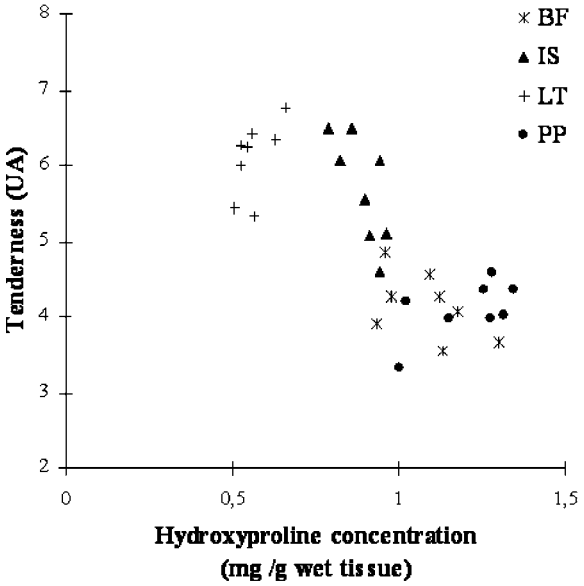

Figure 5. Distribution of the muscle types according to collagen content (hydroxyproline concentration) and sensory tenderness (arbitrary units) and designation of the groups used for the GDA.

images (histolength). This confirms that the two imaging modalities gave complementary information for the prediction of sensory tenderness. The best classification results were obtained with the two variables G_{7-10} and histolength. The model explained 86% of the variance of tenderness, with 100% correct classification for the learning and validation groups and 87.5% for the test group, i.e., a total score of 97% (**Table 3**). According to the mean value of the model predictors, the perimysium network was longer in the tough group than in the tender group (**Table 3**), thus showing that the network of the tougher samples was more branched than that of the more tender ones. Moreover, there were significantly more objects of the G_{7-10} size (radius ranging from 0.7 to 1.0 mm) in the tougher muscles (**Table 3**). This indicates that the total surface occupied by small fiber bundles was greater in this group.

Table 3. Best Model Parameters for Predicting Sensory Tenderness[a]

	mean values in the class (% of total image)			correctly classified (%)		
variables	tough	tender	R^2	learning/ validation ($n = 24$)	test ($n = 8$)	total ($n = 32$)
G_{7-10}	1.87	1.54	0.86	100	87.5	96.9
histolength	0.29	0.16				

[a] Models were obtained by GDA (best subset algorithm) on filtered data. G_{7-10} expressed the total surface occupied by hexagons of the radius between 7 and 10 pixels in MRIs, and histolength is the length of the connective tissue in histological images.

With a one-variable model, the collagen content was the only variable kept and 81% of all samples were correctly classified. Interestingly when the collagen content was entered in a three-variable model, including G_{7-10} and histolength, no improvement was observed in the percentage of explained variance. We concluded that the connective tissue structure measurements already included a large part of the information brought by collagen content in the models for tenderness.

Models to Predict Instrumental Toughness (C80). The C80 toughness value used to divide the data into the two groups was 145 N/cm^2. The tough group included most PP and only two BF samples. The tender group included all of the IS and LT samples and six of the eight BF samples (**Figure 7**).

The one-way ANOVA selected six significant variables ($p < 0.05$) out of 27 on their ability to discriminate the instrumental toughness classes (**Figure 8**). None of the variables measured on the histological images were significant ($p < 0.05$). The best model obtained with GDA best subset algorithm contained three almost consecutive granulometry variables from MR images, i.e., G_{18-21}, G_{7-10}, and G_{11-13} (**Table 4**), with 92% of samples correctly classified in the learning/validation group and only 87.5% correctly classified in the test group. The results for the test group indicate that we must be careful with interpretation. However, on average, G_{18-21} was higher in the tender group, whereas G_{7-10} and G_{11-13} were higher in the tough

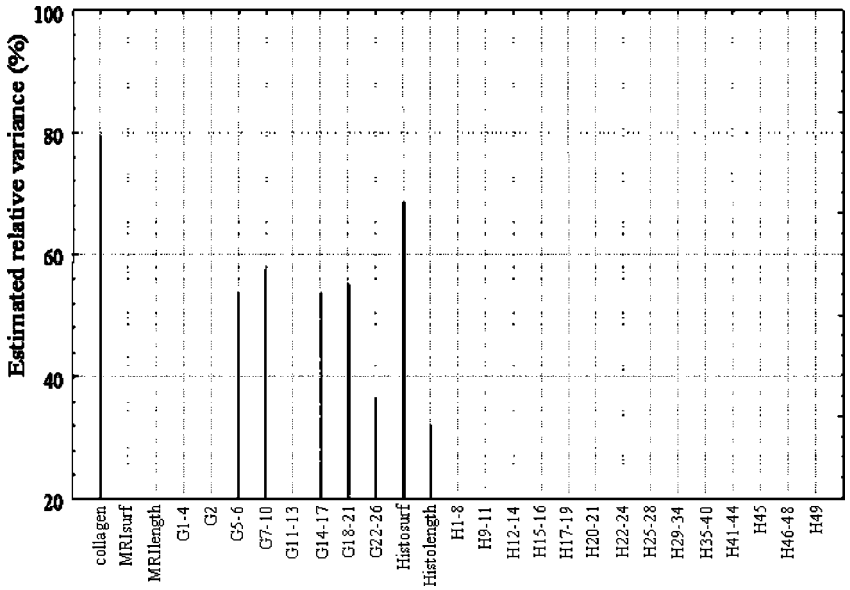

Figure 6. ANOVAgram of the contribution of sensory tenderness factor to the variation of estimated relative variance for each of the 27 variables. A relative variance of 20% was used to determine the significance threshold of the one-way ANOVA ($p < 0.05$). G_{i-j} and H_{i-j} are granulometry variables for NMR and histological images, respectively. MRIsurf, MRIlength and Histosurf, Histolength were the surface and the length of perimysium on MRIs and on histological images, respectively.

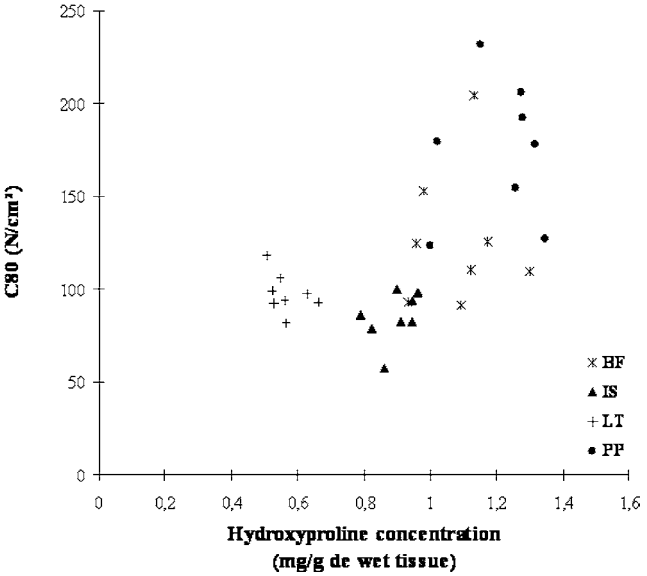

Figure 7. Distribution of the muscle types according to collagen content (hydroxyproline concentration) and instrumental toughness [stress in compression test at 80% of deformation (N/cm^2)] and designation of the groups used for the factorial discriminant analysis.

group (**Table 4**), indicating a greater number of small fascicles and a smaller number of large fascicles in the tough group using the Charolais breed and the muscle types in the present study. G_{14-17} was not significantly different between the tough and the tender samples ($p < 0.05$). The model including only the collagen content led to a lower percentage of correctly classified muscles (75% correctly classified in the test group). The instrumental toughness was more related to the structure of the IMCT visualized by MRI than to collagen content.

Models to Predict Collagen Content. The collagen content value used to divide the data into the two classes was 0.85 mg OH−Pro/g fresh muscle (**Figure 7**). The low collagen group included all LT samples and two IS samples, whereas the high collagen group included all BF and PP samples and six out of the eight IS samples.

The one-way ANOVA selected eight significant variables ($p < 0.05$) out of 26, which enabled the discrimination of the muscle samples according to collagen content class factor (**Figure 9**). The best model obtained by GDA best subset algorithm included the same variables (G_{7-10} and histolength) as those of the model for sensory tenderness prediction (**Table 5**). However, although it led to 96% correctly classified samples in the learning/validation group, only 63% of the test group was correctly classified, despite a R^2 value of 0.80. According to the mean values of the model predictors, the samples classified as having low collagen had a fewer number of small fascicles belonging to the G_{7-10} cluster and a shorter IMCT network group (**Table 5**).

Table 4. Best Model Parameters for Predicting Instrumental Toughness (C80)[a]

	mean values in the class (% of total image)			correctly classified (%)		
				learning/ validation	test	total
variables	tough	tender	R^2	($n = 24$)	($n = 8$)	($n = 32$)
G_{7-10}	0.32	0.23	0.61	91.7	87.5	90.6
G_{11-13}	0.22	0.17				
G_{18-23}	0.03	0.07				

[a] Models were obtained by GDA (best subset algorithm) on filtered data. G_{i-j} expressed the total surface occupied by hexagons of the radius between i and j pixels in MRIs.

The two main objectives of this study were to develop a method of image analysis for the quantification of the IMCT network at the perimysium level and to determine the relationship between structural parameters and cooked meat texture measurements. The granulometry of MR images played a major role in the models predicting the tenderness of our meat samples. These variables were the most discriminating and contributed to all models. They gave information about the macroscopic structure of the perimysium and the size of the delimited fascicles. However, the measurements of the perimysium surface and the length of its network on MR images did not contribute to any model. The IMCT surface was 4-fold greater in the MR images as compared to that in the histology images. The method used for generating MR images of connective tissue (i.e., based on susceptibility contrast) is known to overestimate the thickness

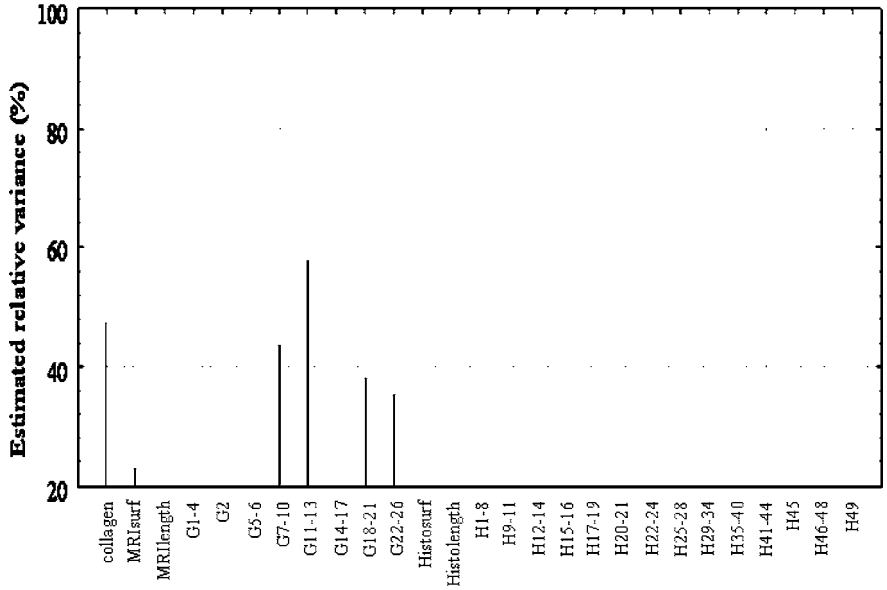

Figure 8. ANOVAgram of the contribution of instrumental toughness factor (C80) to the variation of estimated relative variance for each of the 27 variables. A relative variance of 20% was used to determine the significance threshold of the one-way ANOVA ($p < 0.05$). For the variables designation, see **Figure 6**.

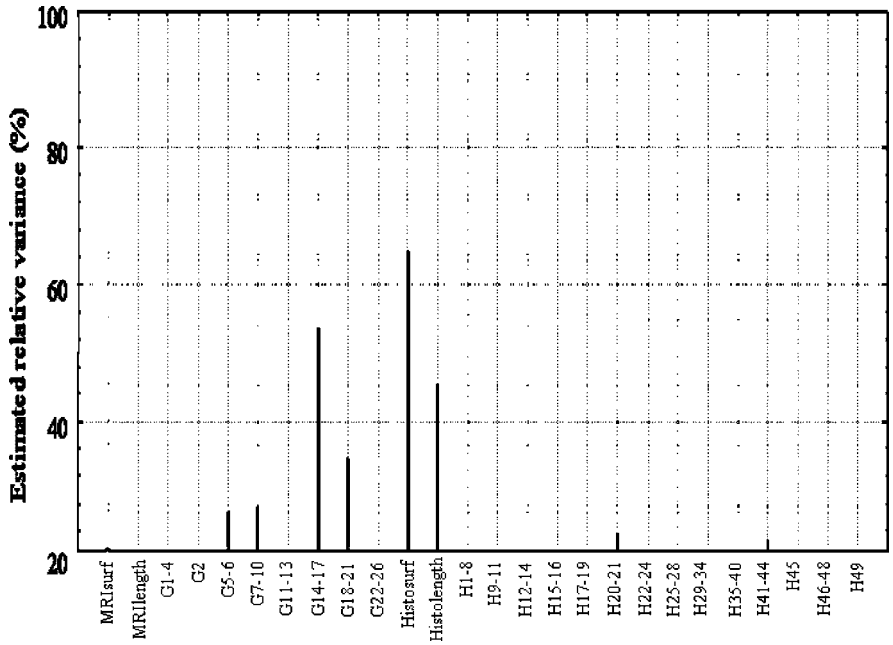

Figure 9. ANOVAgram of the contribution of collagen content factor to the variation of estimated relative variance for each of the 26 variables. A relative variance of 20% was used to determine the significance threshold of the one-way ANOVA ($p < 0.05$). For the variables designation, see **Figure 6**.

Table 5. Model Parameters for Predicting Collagen Content[a]

	mean values in the class (% of total image)			correctly classified (%)		
				learning/ validation	test	total
variables	tough	tender	R^2	($n = 24$)	($n = 8$)	($n = 32$)
G_{7-10}	0.18	0.26	0.80	95.8	62.5	87.5
histolength	1.42	1.83				

[a] Models were obtained by GDA (best subset algorithm) on filtered data. G_{7-10} expressed the total surface occupied by hexagons of the radius between 7 and 10 pixels in MRIs, and histolength is the length of the connective tissue in histological images.

of the network in two ways. First, the contrast allows detecting a small insertion (i.e., the connective tissue) in a bulk matrix (myofibers) even if the size of the insertion is smaller than the voxel volume (*32*). It results in an apparent thickening of the objects, which appear larger than its original size. Second, MRI also detects the lipids (intramuscular fat) and does not provide a signal specific to the collagenic tissue. Indeed, lipids generate a high hyposignal, also leading to an overestimation of the perimysial thickness while their contribution to texture variations is negligible (*20*). This thickening implies a higher error on the thinnest linear objects that were one to a few pixels thick, as compared with the error made on circular objects such as hexagons. Thus, the granulometry measurements on MR images are less distorted than the network measurements.

Some variables from the histological images completed the models. Contrary to the importance of the granulometry in the MRI measurements, for histological images, only the network measurements (length) contributed to the models. The histology granulometry variables were not significantly discriminating for the different class factors, i.e., sensory tenderness, instrumental toughness, and collagen content. They brought information in a narrower field of view about objects of smaller size than NMR granulometry variables. Indeed, H_{49}, the largest granulometry variable used from histological images, corresponded to G_{13} situated in the middle of the granulometry curve of MR images (**Figure 3**). In addition, the small size of the histological samples limited the significance of the large size variables such as H_{35-40}. The fascicles visualized at smaller scales, like those observed on histological images, did not vary morphologically according to the type of muscle and they contributed little to the variations in meat tenderness. When a segmentation extracting the thinner network was performed (a low confidence level, $\epsilon = 40\%$), the models became less efficient (data not shown). Our results thus show that the more the segmentation focused on small fascicles, the less variable and the less related to the tenderness variability.

The best model predicting the instrumental toughness (C80) included only granulometry variables from MR images, whereas the best model predicting sensory tenderness used both MRI and histology variables. Sensory tenderness is a global assessment of meat texture during the mastication process, which includes the progressive and complete degradation of the different levels of structure of the perimysium. Even the thinnest level of perimysium is completely destroyed in the residual bolus. Such a level of destruction was not reached during the compression test. Thus, the information given by the histological images about the thinnest structures was not necessary to explain the C80 variations. Moreover, the histological variables were more related to collagen content than the MRI variables and the correlation between sensory tenderness and collagen content was stronger than the correlation between C80 and collagen content. This is probably why the C80 prediction model did not include the complementary information about collagen content contributed by the histological network variables.

The size of the granulometry variables kept in the models indicated that the macroscopic fascicles of perimysium discriminated tender samples from tough samples better than small fascicles and thin perimysium. G_{7-10} appeared in all models and defined objects with a radius of 0.7−1 mm, i.e., small objects in MRI and large objects at the histological scale. This variable is located at the borderline between the two techniques of imagery used in the present work. Apparently, the number of objects of this size played a major role in determining the tenderness value of our meat samples. Under the conditions of the present study, the tough samples had more fascicles of this size than the tender samples. Our results thus showed that tougher muscles had greater proportions of small macroscopic

muscle fiber fascicles (0.7−1.0 mm radius). This was confirmed by the opposite behavior of G_{18-21}, characteristic of 1.8−2.1 mm radius objects, which represented large fascicles and which were found in higher proportions in the more tender samples. Several previous studies (*7*−*9*) concluded that tender meats have small fiber bundles. All of these authors observed muscle sections by microscopy and characterized primary and secondary fascicles (i.e., the two levels of organization of perimysium above endomysium). At this scale in this study, we found no difference between tender and tough samples. With MRI, the observed structures are only secondary fiber bundles, since this type of imagery allows acquiring images in a much larger field of view. As MRI only showed thick perimysium, the images of tender muscles, like IS and LT, included few segments of perimysium and thus appeared like an open network. The granulometry of the IMCT of these muscles indicated mostly large objects. In contrast, images of the tough muscles, like BF and PP, showed a more defined and more branched network of thick perimysium. Their granulometry measurements indicated more small objects.

In conclusion, the two imaging methods produced complementary information about the IMCT structure, the MRI at the macroscopic level and the histology at a smaller scale. Both levels were necessary to predict sensory tenderness, but only the structure of IMCT observed by MRI was useful to predict instrumental toughness. The present results indicate that, at a macroscopic scale, muscles with small fascicles delimited by a thick primary perimysium are tougher than muscles with large fascicles delimited by a thin primary perimysium. The major influence of macroscopic IMCT structure in predicting tenderness confirms the interest of setting up tools making possible the study of meat samples in large fields of view (whole steaks) with an imaging method simpler than MRI and applicable for on-line measurement. These results have been obtained on meat cooked in conditions (65 °C, 30 min) inducing myofiber and collagen heat denaturation but not extensive collagen contraction. Higher cooking temperatures would have caused a greater increase in myofiber resistance and a decrease in IMCT resistance, which could have had an influence on the respective roles played by the connective tissue network and the myofibers on meat tenderness. Further validation is then required on a larger range of types of muscle and types of animal and also with other cooking conditions to generalize the models developed.

ABBREVIATIONS USED

ANOVA, analysis of variance; BF, *Biceps femoris*; GDA, general discriminant analysis; IMCT, intramuscular connective tissue; IS, *Infraspinatus*; LT, *Longissimus thoracis*; MR, magnetic resonance; MRI, magnetic resonance imaging; PC, principal component; PCA, principal component analysis; PP, *Pectoralis profundus*.

LITERATURE CITED

(1) Boleman, S. J.; Boleman, S. L.; Miller, R. K.; Taylor, J. F.; Cross, H. R.; Wheeler, T. L.; Koohmaraie, M.; Shackelford, S. D.; Miller, M. F.; West, R. L.; Johnson, D. D.; Savell, J. W. Consumer evaluation of beef of known categories of tenderness. *J. Anim. Sci.* **1997**, *75*, 1521−1524.

(2) Obuz, E.; Dikeman, M. E.; Loughin, T. M. Effects of cooking method, reheating, holding time, and holding temperature on beef *Longissimus lumborum* and *Biceps femoris* tenderness. *Meat Sci.* **2003**, *65*, 841−851.

(3) Purslow, P. P. Intramuscular connective tissue and its role in meat quality−A review. *Meat Sci.* **2005**, *70*, 435−447.

(4) Fang, S. H.; Nishimura, T.; Takahashi, K. Relationship between development of intramuscular connective tissue and toughness of pork during growth of pigs. *J. Anim. Sci.* **1999**, *77*, 120−130.

(5) Brooks, J. C.; Savell, J. W. Perimysium thickness as an indicator of beef tenderness. *Meat Sci.* **2004**, *67*, 329−334.

(6) Brady, D. E. A study of the factors influencing tenderness and texture of beef. *Proc. Am. Soc. Anim. Prod.* **1937**, *30*, 246−250.

(7) Ramsbottom, J. M.; Strandine, E. J.; Koonz, C. H. Comparative tenderness of representative beef muscles. *Food Res.* **1945**, *10*, 497−509.

(8) Cooper, C. C.; Breidenstein, B. B.; Cassens, R. G.; Evans, G.; Bray, R. W. Influence of marbling and maturity on the palatability of beef muscle: Histological considerations. *J. Anim. Sci.* **1968**, *27*, 1542−1546.

(9) Norman, G. A. Effects of breed and nutrition on the productive traits of beef cattle in South-East Brazil: Part 3−Meat quality. *Meat Sci.* **1982**, *6*, 7−86.

(10) Liu, A.; Nishimura, T.; Takahashi, K. Relationship between structural properties of intramuscular connective tissue and toughness of various chicken muscles. *Meat Sci.* **1996**, *43*, 43−49.

(11) Bonny, J.-M.; Laurent, W.; Labas, R.; Taylor, R.; Berge, P.; Renou, J.-P. Magnetic resonance imaging of connective tissue: A nondestructive method for characterizing muscle structure. *J. Sci. Food Agric.* **2000**, *81*, 337−341.

(12) Sifre-Maunier, L.; Taylor, R. G.; Berge, P.; Bonny, J.-M. Image analysis for characterization of the intramuscular connective tissue in meat. 50th ICoMST, Helsinki, 2004; p 118.

(13) Dougherty, E. R.; Pelz, J. B. Morphological granulometric analysis of electrophotographic images−Size distribution statistics for process control. *Opt. Eng.* **1981**, *30*, 438−444.

(14) Lepetit, J.; Culioli, J. Mechanical properties of meat. *Meat Sci.* **1994**, *36*, 203−237.

(15) Lepetit, J.; Buffiere, C. Comparaison de deux méthodes mécaniques de mesure de la résistance myofibrillaire de la viande crue. *Viande et Produits Carnés* **1993**, *14*, 39−42.

(16) Cross, H. R.; West, R. L.; Dutson, T. R. Comparison of methods for measuring sarcomere length in beef *Semitendinosus* muscle. *Meat Sci.* **1981**, *5*, 261−266.

(17) Bergman, I.; Loxley, R. Two improved and simplified methods for the spectrophotometric determination of hydroxyproline. *Anal. Chem.* **1963**, *35*, 1961−1965.

(18) Bonnet, M.; Kopp, J. Dosage du collagène dans les tissus conjonctifs, la viande et les produits carnés. *Viandes et Produits Carnés* **1986**, *7*, 263−266.

(19) Statistica software release 6.1, Statsoft, France.

(20) McKeith, F. K.; De Vol, D. L.; Miles, R. S.; Bechtel, P. J.; Carr, T. L. Chemical and sensory properties of thirteen major beef muscles. *J. Food Sci.* **1985**, *50*, 869−872.

(21) Torrescano, G.; Sanchez-Escalante, A.; Gimenez, B.; Roncales, P.; Beltran, J. A. Shear values of raw samples of 14 bovine muscles and their relation to muscle collagen characteristics. *Meat Sci.* **2003**, *64*, 85−91.

(22) Kamoun, M.; Culioli, J. Mechanical behaviour of cooked meat under sinusoidal compression. *J. Text. Stud.* **1988**, *19*, 117−136.

(23) Carmack, C. F.; Kastner, C. L.; Dikeman, M. E.; Schwenke, J. R.; Garcia Zepeda, C. M. Sensory evaluation of beef-flavor-intensity, tenderness, and juiciness among major muscles. *Meat Sci.* **1995**, *39*, 143−147.

(24) Jeremiah, L. E.; Gibson, L. L.; Aalhus, J. L.; Dugan, M. E. R. Assessment of palatability attributes of the major beef muscles. *Meat Sci.* **2003**, *65*, 949−958.

(25) Rhee, M. S.; Wheeler, T. L.; Shackelford, S. D.; Koohmaraie, M. Variation in palatability and biochemical traits within and among eleven beef muscles. *J. Anim. Sci.* **2004**, *82*, 534−550.

(26) Culioli, J. Meat tenderness: Mechanical assessment. In *Expression of Tissue Proteinases and Regulation of Protein Degradation as Related to Meat Quality*; Ouali, A., Demeyer, D. I., Smulders, F. J. M., Eds.; ECCEAMST: Utrecht, The Netherlands; pp 239−266.
(27) Harris, P. V.; Shorthose, W. R. Meat texture. In *Developments in Meat Science*; Lawrie, R. A., Ed.; Elsevier Applied Science: London, 1988; Vol. 4, pp 245−296.
(28) Shackelford, S. D.; Wheeler, T. L.; Koohmaraie, M. Relationship between shear force and trained sensory panel tenderness ratings of 10 major muscles from *Bos indicus* and *Bos taurus* cattle. *J. Anim. Sci.* **1995**, *73*, 3333−3340.
(29) Mathoniere, C.; Mioche, L.; Dransfield, E.; Culioli, J. Meat texture characterisation: Comparison of chewing patterns, sensory and mechanical measures. *J. Text. Stud.* **2000**, *31*, 183−203.
(30) Dransfield, E. Intramuscular composition and texture of beef muscles. *J. Sci. Food Agric.* **1977**, *28*, 833−842.
(31) Jeremiah, L. E.; Dugan, M. E. R.; Aalhus, J. L.; Gibson, L. L. Assessment of the chemical and cooking properties of the major beef muscles and muscle groups. *Meat Sci.* **2003**, *65*, 985−992.
(32) Yablonskiy, D. A.; Haacke, E. M. Theory of NMR signal behavior in magnetically inhomogeneous tissues: The static dephasing regime. *Magn. Reson. Med.* **1994**, *32*, 749−763.

Received for review April 19, 2005. Revised manuscript received July 24, 2005. Accepted July 31, 2005.

JF0508910